REFRACTORY, CERAMIC, AND COMPOSITE MATERIALS

Fabrication, Microstructure and Properties of the Mid-Fraction SiC Particles/6061Al Composites Using an Optimized Powder Metallurgy Technique

Yinqiu Huang[a], Guohong Chen[b], Binhao Wang[a], Jianhua Zhang[a], and Wenming Tang[a], *

[a]*School of Materials Science and Engineering, Hefei University of Technology, Hefei, 230009 China*
[b]*Anhui Electric Power Research Institute, State Grid Corporation of China, Hefei, 230601 China*
*e-mail: wmtang69@126.com

Abstract—Commercial F500 SiC powder and 6061Al powder were chosen to fabricate the mid-fraction SiC particles (SiCp)/6061Al composite of 30 vol % (volume fraction) SiC using a pressureless sintering technique. Decantation of the SiC powder and optimization of the sintering temperature were performed to improve the microstructure and properties of the composite. The results show that near full-densification of the 30 vol % SiCp/6061Al composite sintered at 680°C is achieved, and no SiCp/Al interfacial reaction occurs. The composite possess the following set of properties: relative density of 98.2%, bending strength of 425.6 MPa, thermal conductivity (TC) of 159 W/(m K) and coefficient of thermal expansion (CTE) of $12.5 \times 10^{-6}/°C$ (20–100°C). The fracture of the composite occurs via cleavage of the SiC particles and ductile tearing of the Al alloy matrix, indicating a strong SiCp/Al interface bonding.

Keywords: SiCp/Al composite, pressureless sintering, microstructure, mechanical properties, thermophysical properties

1. INTRODUCTION

SiC particles (SiCp)/Al composites are generally regarded as important structural materials in the areas of aerospace engineering, precision instruments, automobile engineering, etc., due to their low density, high thermal conductivity (TC), specific strength and stiffness, controllable coefficient of thermal expansion (CTE) and excellent wear resistance properties. More importantly, these composites of mid/high SiC fractions are successfully used as a kind of new-generation electronic packaging material [1]. A series of SiCp/Al electronic packaging composites have been developed by the world-leading Thermal Transfer Corporation (TTC, Duquesne, PA, USA), using pressureless infiltration (PRIMEX™) and also stirring cast (PRIMEX Cast™) technologies [2]. They are being successfully commercialized, due to their perfect mechanical and thermophysical properties. However, machining of the composites, including cutting, grinding and drilling, is actually required to produce the electronic packaging cases of complicated shape and/or thin walls, which is time-consuming and costly. Even worse, severe surface damage of the electronic packaging cases occurs during the machining process, e.g., fragmentation of the SiC particles and their interfacial separation from the Al alloy matrix [3]. As a result, the mechanical and thermophysical properties, and microstructure of the composite cases are dramatically affected. Accordingly, it is

necessary to develop alternative technologies to fabricate the mid/high-fraction SiCp/Al composites, in order to reduce the amount of machining of the electronic packaging cases as much as possible.

Until now, pressureless infiltration and stir casting have been the most-frequently used methods to produce the high and low fraction SiCp/Al composites [2, 4]. However, when the mid-fraction SiCp/Al composites of 20–40 vol % SiC are fabricated using such techniques, the problem with the SiC preform preparation for pressureless infiltration and uniform distribution of the SiC particles for stir casting in the composites is that they are hard to handle. Comparatively, powder metallurgy can provide a good solution, which is particularly suitable for fabricating products of small size and complex shape without much machining. Furthermore, the technique also has unique advantages in producing the SiCp/Al electronic packaging composites: (1) ensures uniform distribution of the SiC particles in the Al matrix and conveniently tailoring of the composite composition as needed, and (2) effectively restrains the negative interfacial reactions due to low sintering temperature. Accordingly, the fabrication of the mid/high-fraction SiCp/Al composites *via* powder metallurgy has received growing attention.

During powder metallurgy of the mid-fraction SiCp/Al composites, the uniform distribution of the SiC particles depends on the content and size of

the SiC particles in the composites. According to the report by Jayakumar et al. [5], when the SiC content is less than 15 vol %, the SiC particles distribute uniformly in the SiCp/356Al composites. However, as the SiC content is increased to 20 vol % and higher, they apparently agglomerate. Mechanical alloying is usually employed for mixing the mid/high-fraction SiCp/Al composite powders, but SiC particles are easily fragmented during ball milling to produce finer SiC particles. The aggravated agglomeration of SiC particles inevitably brings about several negative effects, such as the increased in porosity, the decrease in the SiCp/Al interfacial bonding strength and thus the degradation of the mechanical and thermophysical properties of the composites [6]. Hao et al. [7] reported that the ratio between the particle size (*RPS*) of Al alloy and SiC powders had a great effect on the microstructure and tensile properties of the 2.4–27.6 vol % SiCp/2014Al composites. The highest density and tensile strength are achieved when the *RPS* of the composites is a little bit smaller than 1. Moreover, several studies have confirmed that high purity N_2 is the most suitable ambient atmosphere for sintering the Al alloys and the SiCp/Al composites [8]. Even so, the properties of the SiCp/Al composites fabricated *via* powder metallurgy are hitherto lower than those of the composites prepared *via* the pressureless/pressure infiltration.

Among the various powder metallurgy routes, pressureless sintering is not only the simplest and most cost-effective one, but also has obvious advantages in fabricating the products with complicated shape, compared with other special powder metallurgy routes, such as hot pressing, spark plasma sintering and hot extrusion/rolling. However, the reported literature on pressureless sintering of the SiCp/Al composites is limited, to date, possibly due to their undesirable microstructure and properties.

Recently, a liquid-phase pressureless sintering technique was successfully employed to prepare the high-fraction SiCp/Al composite of 50 vol % SiC [9]. It needs to be verified whether such a powder metallurgy technique is suitable for the mid-fraction SiCp/Al composite or not. The SiC content is less, and thus the distribution of the SiC particles is discontinuous in the mid-fraction SiCp/Al composite, so, the liquid-phase sintering temperature must be strictly controlled in case that the Al alloy melt leaks from the sintered bodies. In this article, a 30 vol % SiCp/6061Al composite was fabricated *via* the modified method, with the aim of developing a novel low-cost technology for manufacturing mid-fraction SiCp/Al composites. Additionally, the microstructure and properties of the composite were also investigated.

2. EXPERIMENTAL

The atomized 6061Al alloy powder and F500 SiC powder are used as raw materials. The purity of the SiC powder is over 98 wt %, and the chemical composition of the Al alloy powder is shown in Table 1. The Al alloy powder has an average particle size (d_{50}) of 15 μm. The

Table 1. Chemical composition of the 6061Al alloy powder (wt %)

Mg	Si	Fe	Cu	Mn	Zn	Al
0.975	0.59	0.092	0.289	0.08	0.031	Bal.

SiC powder has a very narrow particle size distribution, d_{50} of the powder is 16 um, measured on a Mastersizer 2000 type laser powder particle size analyzer (Fig. 1). The *RPS* of the 6061Al alloy and SiC powders is slightly below 1 (0.94), which is beneficial for the sintering densification of the SiCp/6061Al composite [7].

The SiC powder was added into deionized water and the mixture was ultrasonicated for 10 min and subsequently left to stand for 20 min. Then, the small SiC particles suspended in water were poured off. This process was repeated two or three times. After decantation, the SiC powder was dried at 150°C for 12 h and then blended with the 6061Al powder at a volume ratio of 30 : 70. Five-mm diameter ZrO_2 balls were used as the milling agent and the ball to powder mass ratio was set to 2 : 1. Mixing of the 30 vol % SiCp/6061Al powder was performed in a bi-roller mixer at a rotating speed of 500 r/min. The mixing time was fixed at 12 h. Afterwards, 1 wt % solid paraffin was added into the powder mixture as the forming agent, and stirred constantly for 2 h in a water bath heated at 85°C. The powder mixture was then poured into the steel mold coated by a thin zinc stearate layer and uniaxially pressed under 600 MPa for 1 min using a 769YP-40C type powder compressing machine. The compacts were placed in a corundum boat and covered with the 6061Al and SiCp powder mixture. The compacts were pressureless sintered using an OTF-1200X type tube furnace. The sintering temperature was set at 660, 680, and 700°C, separately, which are all higher than the liquidus temperature of the 6061Al alloy (652°C). The samples were heated from room temperature to 350°C at a rate of 3°C/min and held at that temperature for 60 min to remove the wax from them. Then, they were heated to the set sintering temperature at a rate of 2°C/min and held for 120 min. Finally, the samples were cooled to 300°C at a rate of 2°C/min and then naturally cooled. The whole sintering process was protected in a 99.999 vol % high-purity N_2 atmosphere at a flow rate of 100 mL/min.
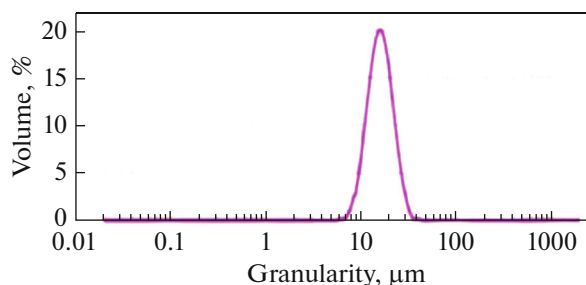

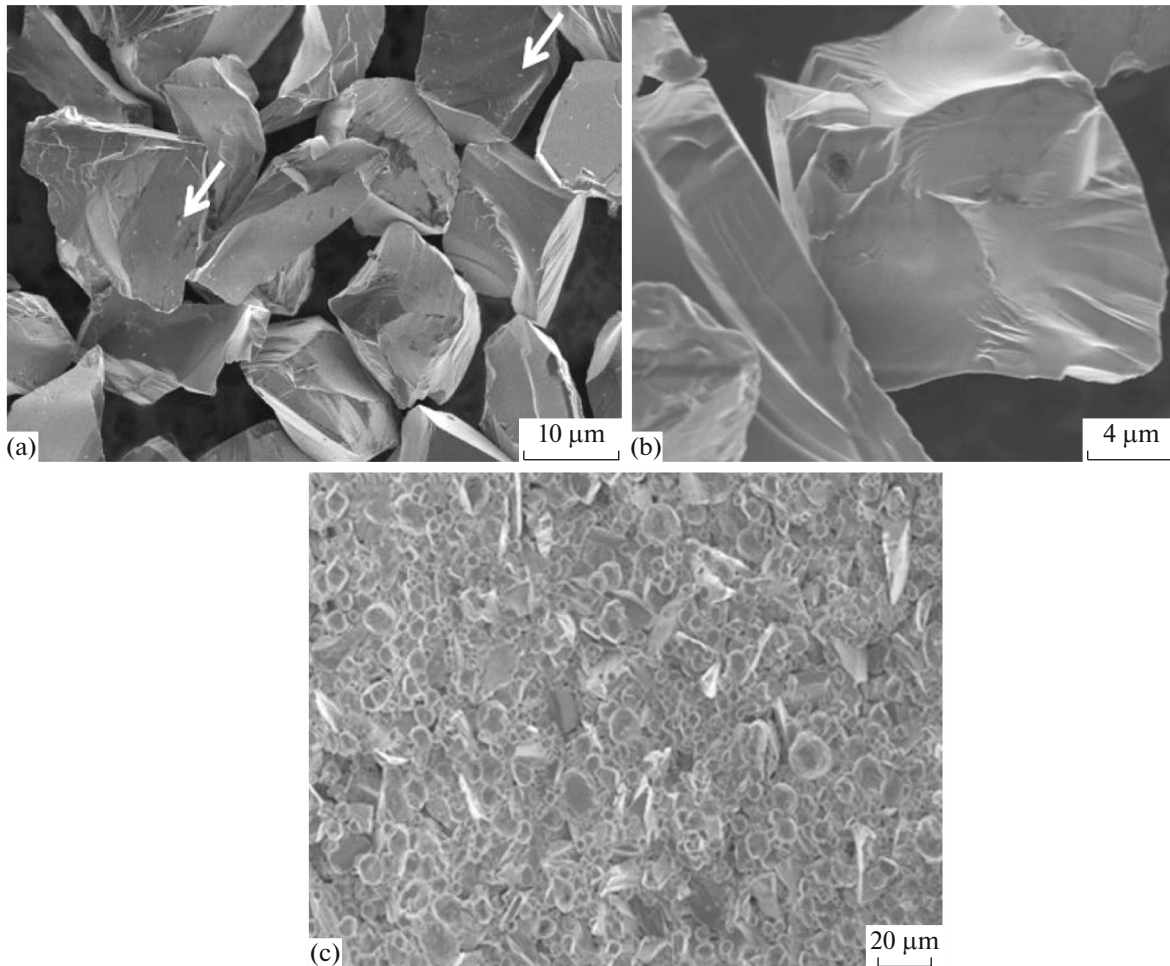**Fig. 1.** Particle size distribution of the SiC powder.

Fig. 2. Scanning electron microscopy (SEM) images showing the morphology of the SiC powder and fractograph of the 30 vol % SiCp/6061Al compacts (a) F500 SiC powder; (b) As-decantated F500 SiC powder; (c) Fractograph of the compacts.

The density of the 30 vol % SiCp/6061Al composite was measured by the Archimedes method, using a FA2004 N electronic balance with a precision of 0.1 mg (Tianping Instrument Co., Ltd., Shanghai, China). The phases of the composite were analyzed by X-ray diffraction (XRD) with a D/MAX2500V X-ray diffractometer (Rigaku Corp, Tokyo, Japan) using Cu $K\alpha$ radiation and the tube voltage and current of 20 kV and 200 mA, respectively. The scanning rate was set to 3°/min and the scanning range was from 10° to 90°. The fracture surface morphologies of the composite were observed by field emission scanning electron microscopy (FESEM) on a SU8020 field emission scanning electron microscope (Hitachi, Corp., Tokyo, Japan). Samples of 50 mm × 4 mm × 3 mm in size were used in the bending strength test, following the China national standard GB/T 6569-2006. The test was operated using a CMT5105 model microcomputer control electronic universal testing machine (MTS Systems (China) Co., Ltd., Shanghai, China) with a testing span of 32 mm and a beam displacement rate of 0.5 mm/min. The thermal diffusion coefficient (α) of the $\varnothing$12.7 mm × 3 mm disc-shaped sample was tested using a LFA457

laser thermal conductivity tester. The TC of the composite (K_c) was then calculated as follows:

$$K_c = \alpha\rho c_p,$$

where ρ is the density and c_p is the heat capacity of the composite at constant pressure. According to the rule of mixtures (ROM), the c_p value of the 30 vol % SiCp/6061Al composite was calculated as 0.87 J/(g K). The CTE of the composite samples of 5 × 5 × 25 mm in size was tested using a TMA402F3 thermal mechanical analyzer (NETZSCH Scientific Instruments, Germany) under a N_2 atmosphere at a flow rate of 20 mL/min. The test temperature ranged from room temperature to 500°C at a heating rate of 5°C/min.

3. RESULTS AND DISCUSSION

3.1. Morphology of the SiC Powder and Green Body

In the F500 SiC powder, there are plenty of ultrafine SiC particles adhered on the large multi-angular SiCp surfaces, as indicated by the arrows in Fig. 2a. The ultrafine SiC particles have much higher reaction
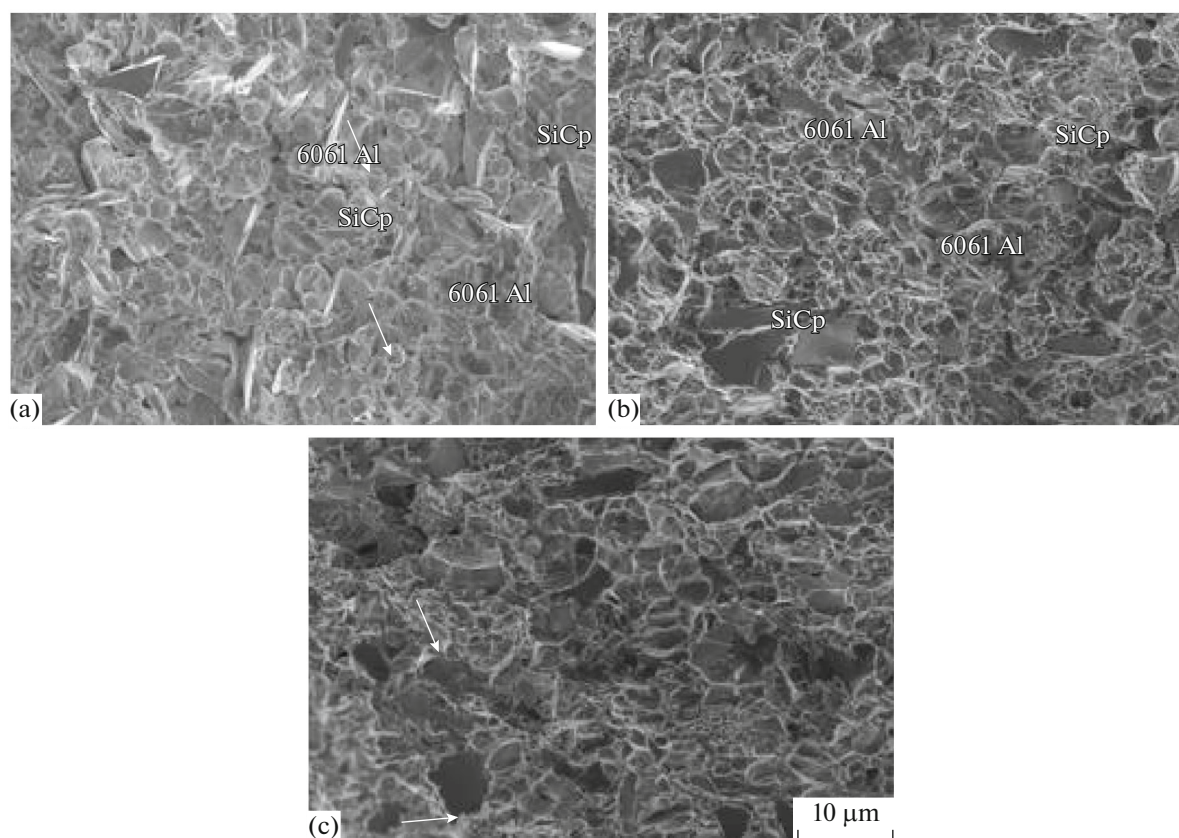
Fig. 3. Scanning electron microscopy (SEM) fractographs of the 30 vol % SiCp/6061Al composite sintered at different temperatures: (a) 660; (b) 680; (c) 700°C.

reactivity with the 6061Al alloy to form more reaction products, than the large SiC particles. After ultrasonic decantation, the ultrafine SiC particles are separated and removed from the large SiCp surfaces (Fig. 2b).

The densification of the SiCp/Al compacts is performed through rearrangement of the SiC and Al alloy particles and also the plastic deformation of the Al alloy particles during the cold-pressing process [10]. Relative density as high as 84% is achieved for the 30 vol % SiCp/6061Al compacts pressed at 600 MPa, and the SiC particles are also randomly distributed in them, though the plastic deformation of the 6061Al particles is not evident (Fig. 2c).

3.2. Microstructure

After pressureless sintering at 660−700°C, the sintered 30 vol % SiCp/6061Al composite is dense without large pores, indicating that the composite has a high sinterability (Fig. 3). The SiC particles are uniformly distributed within the 6061Al matrix without any agglomeration and maintain their originally polygonal shape. The relative density of the 30 vol % SiCp/6061Al composite increased from 94.3 to 98.2%, as the sintering temperature increased from 660 to 680°C, and then, decreased to 96.8%, as the

sintering temperature further increased to 700°C (Fig. 6). In the 660°C sintered composite, numerous micropores with dispersive distribution in the Al alloy matrix, indicating the under-sintering of the composite. As for the 700°C sintered composite, the residual pores preferentially situate at the SiCp/Al alloy interface, as indicated by the arrows in Fig. 3c. Comparatively, the 680°C sintered composite is near-fully dense, with only a few pores present in the Al alloy matrix and/or at the SiCp/Al alloy interface (Fig. 3b). As a contrast, the relative density of the supersolidus liquid-phase sintered (SLPS) 27 vol % SiCp/6061Al composite is only 87% [11], although it has a SiC content similar to the composite sintered at 680°C in this study.

In this study, the chosen sintering temperature was 660°C and above, aiming at implementing the liquid-phase sintering of the composite. As the composite was sintered at 660°C, superheating of the Al alloy is so limited, the following phenomena may arise: (1) the 6061Al particles are not molten; (2) even if the Al alloy inside the 6061Al particles is molten, the melt cannot break through the continuous Al_2O_3 layer around the particles and (3) even if part of the Al alloy particles are molten, the Al alloy melt cannot fill up the pores among the Al alloy particles due to its high viscosity at
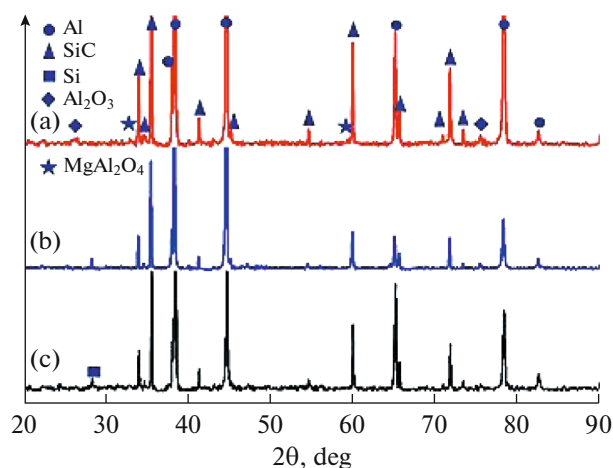
Fig. 4. X-ray diffraction (XRD) patterns of the 30 vol % SiCp/6061Al composite sintered at different temperatures (a) 660; (b) 680; (c) 700°C.

low temperature. More specifically, the viscosity of the Al alloy melt changes from 2.51×10^{-3} Pa s at 665°C to 1.59×10^{-3} Pa s at 705°C [12]. Therefore, the 30 vol % SiCp/6061Al composite sintered at 660°C has the lowest density. In the 30 vol % SiCp/6061Al composite sintered at 680°C, the Al alloy powder is molten completely to form the Al alloy melt of low viscosity. The melt can fill up the gaps among the SiC particles and contact tightly with the SiCp under the compressive stress arising from the CTE mismatch between the 6061Al alloy and SiC. As a result, the composite has the highest density. When the sintering temperature of the composite is increased to 700°C, the viscosity of the Al alloy melt is too low to stably stay in the gaps among the SiC particles. Leakage of the Al alloy melt results in the decrease of the density of the 30 vol % SiCp/6061Al composite. The leakage of the Al alloy melt does not occur in the 50 vol %

SiCp/6061Al composite sintered at the same temperature [9]. The SiC particles construct a continuous three-dimensional frame in which the Al alloy melt is locked, so, leakage of the Al alloy melt in the 50 vol % SiCp/6061Al composite is almost forbidden during sintering at 700°C.

As shown in Fig. 4, beside the intensive diffraction peaks of Al and SiC, weak Al_2O_3 diffraction peaks are present in the XRD pattern of the 660°C sintered composite (Fig. 4a). The Al_2O_3 impurity may originate from the oxide membrane on the 6061Al alloy powder. In the composite sintered at 680°C and above, the amount of Al_2O_3 impurity is reduced, because it partly reacts with the active Mg atoms in the 6061Al melt to form $MgAl_2O_4$ [13]. No Al_4C_3 was detected even in the composite sintered at 700°C, indicating a weaker SiC/Al interface reaction in the composite compared with the composite of 50 vol % SiC [9], due to its lower SiC content. A similar result was reported by Liu et al., when developing the 35 vol % SiCp/2024Al composite by hot pressing [14]. However, the Al_4C_3 phase was found in the 620°C hot-pressed 15 wt % SiCp/2009Al composite developed by Jin et al. [15]. The formation of Al_4C_3 results from the ultrafine SiC powder (7 μm) of a high reactivity with the Al alloy matrix. As shown in Fig. 5, Si particles are embedded in the Al alloy matrix without contact with the SiC particles. They may be originated from crystallization in the Al alloy melt. Thus, the amount of Si reflected by the diffraction peak intensity of Si increases with the sintering temperature (Figs. 4b and 4c).

3.3. Bending Strength

As shown in Fig. 6, the bending strength of the composite increases from 242.1 to 425.6 MPa, as the sintering temperature rose from 660 to 680°C. However, it fell to 417 MPa for the composite sintered at 700°C. The bending strength of the composite has the
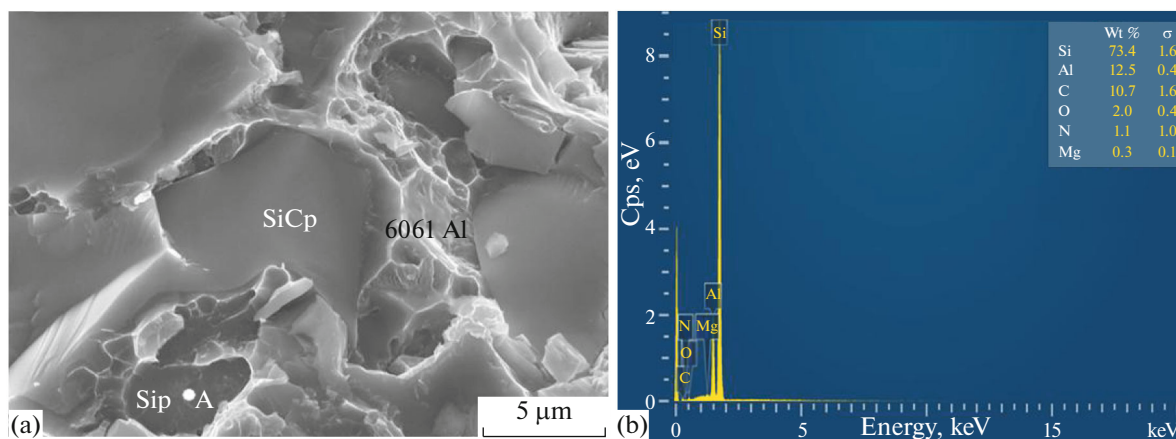

Fig. 5. High-magnification fractograph showing the SiCp/6061Al interface in the 30 vol % SiCp/6061Al composite sintered at 680°C (a) and (b) Energy-dispersive X-ray spectroscopy (EDS) spectrum of point A in Fig. 5a.
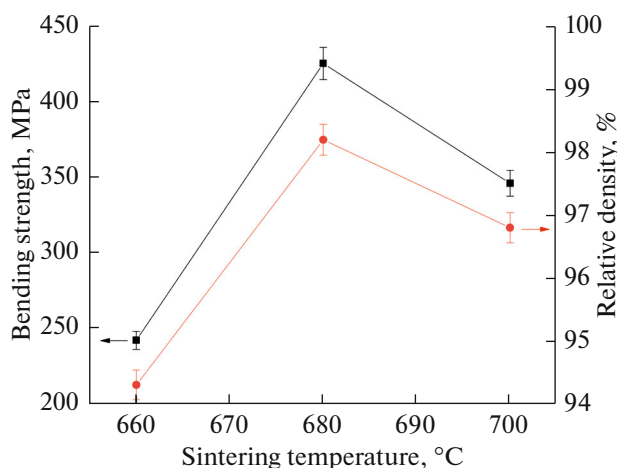
Fig. 6. Relationships of the relative density and bending strength of the 30 vol % SiCp/6061Al composite vs. sintering temperature.

Fig. 7. Relationships of the CTE of the 30 vol % SiCp/6061Al composite vs. test temperature.

same tendency as the relative density of the composite *vs.* the sintering temperature, suggesting that the sintering densification is the crucial factor for the mechanical properties of the composite. As reported by Padmavathi et al. [16], the relative density and bending strength of the 630°C vacuum pressureless-sintered SiCp/6711Al composites decrease with the increasing content of SiCp. The bending strength of the 20 vol % SiCp/6711Al composite is only 215 MPa, about half that of the 30 vol % SiCp/6061Al composite in this study. This can possibly be attributed to the unsatisfactory particle size ratio (*RPS* = 2.16) and extremely low relative density (90.5%) of the SiCp/6711Al composites.

Sintering of the 30 vol % SiCp/6061Al composite is not completed at 660°C, parts of the Al alloy particles in them are still spherical, as indicated by the arrows in Fig. 3a. Additionally, the SiCp/Al interfacial bonding of the composite is rather low. The fracture of the composite preferentially follows an intergranular fracture mode (Fig. 3a). In the composite sintered at 680 and 700°C, ductile tearing of the Al alloy matrix results in the formation of high-density equiaxial dimples. Also, almost all the SiC particles fracture in a cleavage mode (Figs. 3b, 3c and 5a).

3.4. Thermal Conductivity

The TCs of the 30 vol % SiCp/6061Al composite sintered at 660, 680, and 700°C were determined to be 134, 159 and 142 W/(m K), respectively. Since the 680°C sintered 30 vol % SiCp/6061Al composite has the highest relative density and the optimal SiCp/Al interface, the scattering effect of the pores and the SiCp/Al interfaces on the migration of phonons and free electrons in the composite is decreased to the maximum extent. As a result, the TC of the composite is the highest.
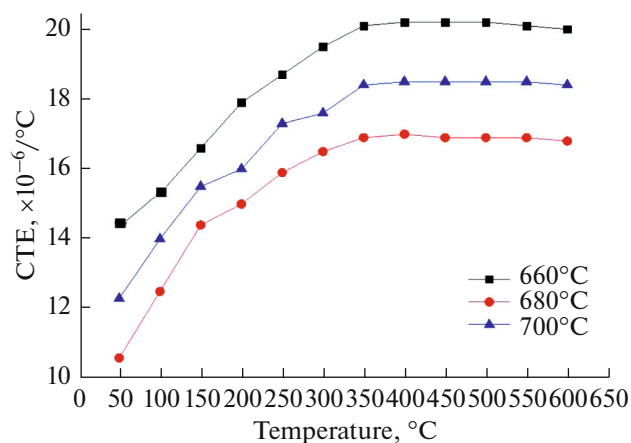
The TC of the 20−40 vol % SiCp/Al composites fabricated using the PRIMEX Cast™ technology varies from 132 to 183 W/(m K) [2]. Accordingly, the TC of the 30 vol % SiCp/Al composite is estimated to be 157 W/(m K), according to the ROM rule. Also, while the 30 vol % SiCp/6061Al composite in this study has the same TC value as the as-cast ones, they are superior to other composites produced by powder metallurgy. For example, the TC of the 45 vol % SiCp/Al composite fabricated by plasma spraying deposition and subsequent hot rolling is only 98.2 W/(m K) [17].

3.5. Coefficient of Thermal Expansion

The CTE of the SiCp/Al composites depends on the characteristics and content of SiC particles, as well as the density and interfacial structure of the composites. As shown in Fig. 7, the CTE of the 680°C sintered 30 vol % SiCp/6061Al composite is the lowest, as the composite has the highest relative density and perfect interfacial structure. As a result, the SiC particles have the most intensive restraining effect on the thermal expansion of the composites. It has been reported that the CTE of the 25 vol % SiCp/2124Al composite and that of 40 vol % SiCp/6092Al composite fabricated by hot pressing are 15.5×10^{-6}/°C and 12.1×10^{-6}/°C (20−100°C), respectively [18]. Similarly, Hao et al. [19] also reported that the CTE of the 40 vol % SiCp/Al composite fabricated by vacuum hot pressing is 11.6×10^{-6}/°C (20−100°C). All these CTE values are approximately equal to the CTE of the 680°C sintered 30 vol % SiCp/6061Al composite (12.5×10^{-6}/°C (20−100°C)) determined in the current study. Furthermore, the CTE of the 20−40 vol % SiCp/Al composites developed by TTC employing the PRIMEX Cast™ technology ranges from 11.9 to 16.2×10^{-6}/°C (20−100°C) [2]. Thus, the CTE of the 680°C sintered 30 vol % SiCp/6061Al composite falls well within this range.

4. CONCLUSIONS

(1) Near full-densification of the 30 vol % SiCp/6061Al composite can be implemented using pressureless sintering at 680°C, in which the SiC particles distribute randomly in the Al alloy matrix, with no apparent SiCp/Al interfacial reaction.

(2) The bending strength and TC of the 30 vol % SiCp/6061Al composite change with the sintering temperature. The 680°C sintered composite has the highest bending strength of 425.6 MPa. The fracture of the composite occurs *via* cleavage of the SiC particles and ductile tearing of the Al alloy matrix, indicating a strong SiCp/Al interface bonding.

(3) The 680°C sintered 30vol% SiCp/6061Al composite has a high TC of 159 W/(m K) and a low CTE of 12.5×10^{-6}/°C (20–100°C), indicating that it can adequately serve as a novel electronic packaging material.

ACKNOWLEDGMENTS

CONFLICT OF INTEREST

The authors claim that they have no conflict of interest.

REFERENCES

1. Ma, P., Wei, Z.J., Jia, Y.D., Yu, Z.S., Prashanth, K.G., Yang, S.L., Li, C.G., Huang, L.X., and Eckert, J., Mechanism of formation of fibrous eutectic Si and thermal conductivity of SiCp/Al–20Si composites under high pressure, *J. Alloys Compd.*, 2017, vol. 709, pp. 329–336.

2. *Thermal Transfer Composites*, http://www.thermaltc.com/products.html, accessed April 15, 2017.

3. Fang, M., Hu, L., Yang, L., Shi, C.D., Wu, Y.C., and Tang, W.M., Electroless plating and growth kinetics of Ni–P alloy film on SiCp/Al composite with high SiC volume fraction, *Trans. Nonfer. Met. Soc. China*, 2016, vol. 26, pp. 799–805.

4. Wang, D.M., Zheng, Z.X., Lv, J., Xu, G.Q., Zhou, S.A., Tang, W.M., and Wu, Y.C., Enhanced thermal conductive 3D-SiC/Al–Si–Mg interpenetrating composites fabricated by pressureless infiltration, *Ceram. Inter.*, 2017, vol. 43, pp. 1755–1761.

5. Jayakumar, K., Mathew, J., Joseph, M., Kumar, R.S., Shukla, A.K., and Samuel, M.G., Synthesis and characterization of A356–SiC composite produced through vacuum hot pressing, *Adv. Manuf. Proc.*, 2013, vol. 28, pp. 991–998.

6. Gui, M., Kang, S.B., and Euh, K., Thermal conductivity of Al–SiCp composites by plasma spraying, *Scr. Mater.*, 2005, vol. 52, pp. 51–56.

7. Hao, S. and Xie, J., Tensile properties and strengthening mechanisms of SiCp-reinforced aluminum matrix composites as a function of relative particle size ratio, *J. Mater. Res.*, 2013, vol. 28, pp. 2047–2055.

8. Pieczonka, T., Schubert, T., Baunack, S., and Kieback, B., Dimensional behaviour of aluminium sintered in different atmospheres, *Mater. Sci. Eng. A*, 2008, vol. 478, pp. 251–256.

9. Mao, X.Z., Hong, Y., Wang, B.H., Liu, J.W., Zhang, Y.J., Feng, D., Yang, L., Shi, C.D., Wu, Y.C., and Tang, W.M., Fabrication, microstructures and properties of 50vol%SiC/6061Al composites via a pressureless sintering technique, *Powder Metall.*, 2018, vol. 61, pp. 1–9.

10. Hafizpour, H.R. and Simchi, A., Investigation on compressibility of Al–SiC composite powders, *Powder Metall.*, 2008, vol. 51, pp. 217–223.

11. Asgharzageh, H. and Simichi, A., Supersolidus liquid phase sintering of Al6061/SiC metal matrix composites, *Powder Metall.*, 2009, vol. 52, pp. 28–35.

12. Kang, Z.C., Mao, D.H., and Deng, J.L., The study of measuring molten aluminium viscosity, *Hunan Nonfer. Met.*, 2001, vol. 17, pp. 18–20.

13. Wang, R.M., Surappa, M.K., Tao, C.H., and Li, C.Z., Microstructure and interface structure studies of SiCp-reinforced Al(6061) metal-matrix composites, *Mater. Sci. Eng. A*, 1988, vol. 254, pp. 219–226.

14. Liu, P., Wang, A.Q., Xie, J.P., and Hao, S.M., Characterization and evaluation of interface in SiCp/2024 Al composite, *Trans. Nonfer. Met. Soc. China*, 2015, vol. 25, pp. 1410–1418.

15. Jin, P., Xiao, B.L., Wang, Q.Z., and Hao, S.M., Effect of hot pressing temperature on microstructure and mechanical properties of SiC particle reinforced aluminum matrix composites, *Acta Metall. Sin.*, 2011, vol. 47, pp. 1025–1037.

16. Padmavathi, C. and Upadhyaya, A., Densification, microstructure and properties of supersolidus liquid phase sintered 6711Al–SiC metal matrix composites, *Sci. Sinter.*, 2010, vol. 42, pp. 363–382.

17. Euh, K.J. and Kang, S.B., Effect of rolling on the thermo-physical properties of SiCp/Al composites fabricated by plasma spraying, *Mater. Sci. Eng. A*, 2005, vol. 395, pp. 47–52.

18. Liu, Y.Q., Fan, J.Z., Sang, J.M., and Shi, L.K., Development of metal matrix composites by powder-metallurgy processing, *Mater. Rev.*, 2010, vol. 24, pp. 18–23.

19. Hao, S.M., Xie, J.P., Wang, A.Q., Wang, W.Y., Li, J.W., and Sun, H.L., Thermal expansion and mechanical properties of middle reinforcement content SiCp/Al composites fabricated by PM technology, *J. Wuhan Univ. Technol. Mater. Sci. Ed.*, 2014, vol. 29, pp. 660–664.